ADVANCED MATERIALS

Supporting Information

for *Adv. Mater.*, DOI: 10.1002/adma. **201104398**

Enhancement of Ferroelectric Polarization Stability by Interface Engineering

*H. Lu , X. Liu , J. D. Burton , C.-W. Bark , Y. Wang , Y. Zhang , D. J. Kim , A. Stamm , P. Lukashev , D. A. Felker , C. M. Folkman , P. Gao , M. S. Rzchowski , X. Q. Pan , C.-B. Eom , E. Y. Tsymbal , and A. Gruverman **

Supplementary Materials

Enhancement of Ferroelectric Polarization Stability by Interface Engineering

H. Lu,[1] X. Liu,[1] J. D. Burton,[1] C.-W. Bark,[2] Y. Wang,[1] Y. Zhang,[3] D. J. Kim,[1] A. Stamm,[1] P. Lukashev,[1] D. A. Felker,[4] C. M. Folkman,[2] P. Gao,[3] M. S. Rzchowski,[4] X. Q. Pan,[3] C.-B. Eom,[4] E. Y. Tsymbal,[1] and A. Gruverman[1]

The switching behavior of the reference $SrRuO_3/BaTiO_3/SrRuO_3$ heterostructure, labeled as no-STO in Fig S1a has been compared with he switching in the $SrRuO_3/SrTiO_3/BaTiO_3/SrTiO_3/SrRuO_3$ heterostructure where both top and bottom interfaces have been engineered by introducing a 2 u.c.-thick $SrTiO_3$ layer between $BaTiO_3$ and $SrRuO_3$ layers (both-STO in Fig S1a). Introduction of the $SrTiO_3$ layer both at top and bottom interfaces results in the 4-fold increase in the remanent polarization value compared with the reference sample (Fig S1b). In other words, modification of both interfaces produces the same effect as modification of only the top interface (Figure 3b in the main paper). This finding confirms that the main mechanism behind the polarization retention enhancement is the change in termination structure at the top interface.

Figure S2 shows EFM images of the reference and both-STO samples after +/-4 V poling. It can be seen that poling of the reference $SrRuO_3/BaTiO_3/SrRuO_3$ sample does not lead to any contrast change, while the same poling procedure performed on the both-STO sample results in the appearance of strong reversible EFM contrast suggesting induction of the screening charge in the electrode.

Figure S3 shows pulse sets used for measurements of the non-switching and switching parts of the polarization loops, pulse set 1 and 2, respectively. Pulse set 1 contains a positive

rectangular preset pulse (1.5 V, 10 ms) followed 1 s later by a triangular positive pulse (1.5 V, 2 ms) to measure a non-switching (loading) current signal. Application of a triangular positive pulse after a negative preset pulse of set 2 allows measurements of the switching current signal along with the loading current signal. The remanent polarization loop was obtained as a difference between signals due to pulse set 2 and 1.

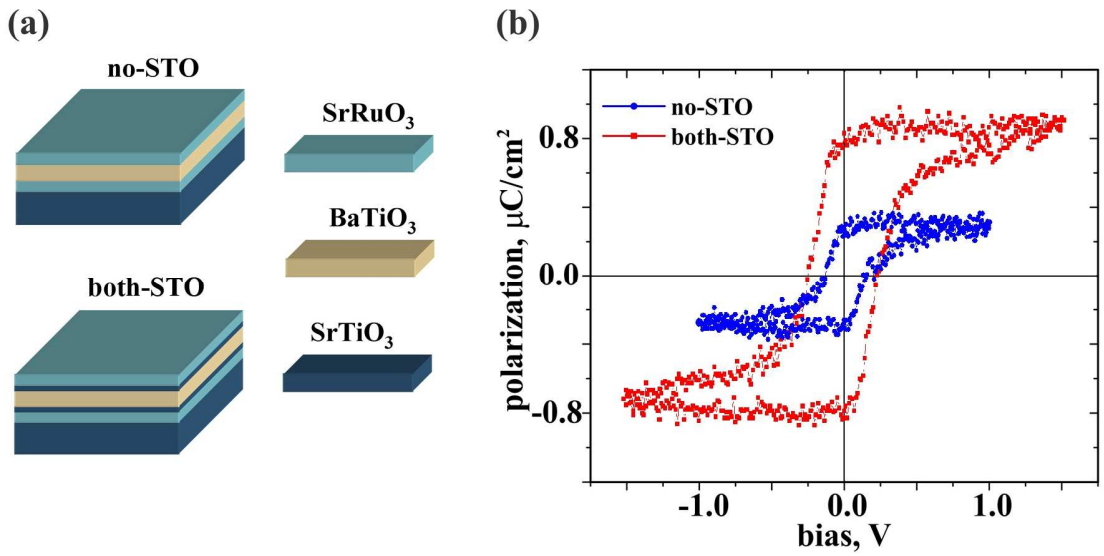

Figure S1. (a) Schematic diagrams of the reference $SrRuO_3/BaTiO_3/SrRuO_3$ structure (no-STO) and a heterostructure with engineered top and bottom interfaces (both-STO). Thickness of the $BaTiO_3$ and $SrTiO_3$ layers is 24 u.c. and 2 u.c., respectively. (b) Remanent P-V hysteresis loops measured by pulsed testing in no-STO, and both-STO heterostructures. Note an almost 300% increase in the remanent polarization for the both-STO sample in comparison with the no-STO sample.

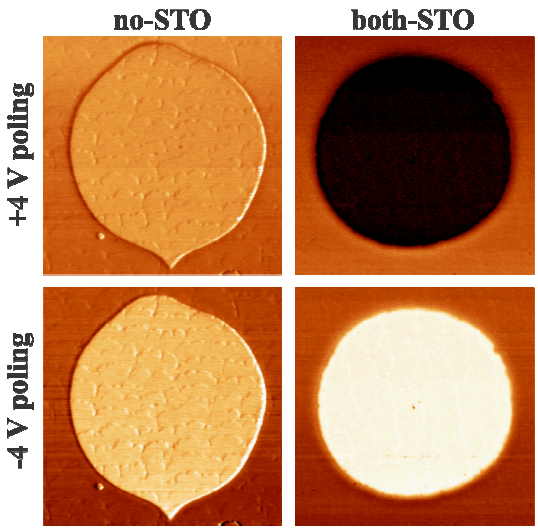

Figure S2. EFM images of the no-STO and both-STO heterostructures after poling by +/-4V pulses. Contrast inversion upon the change of the pulse polarity in the both-STO sample is attributed to the change of screening charge on the electrodes and indicates a presence of a switchable polarization with two stable states.

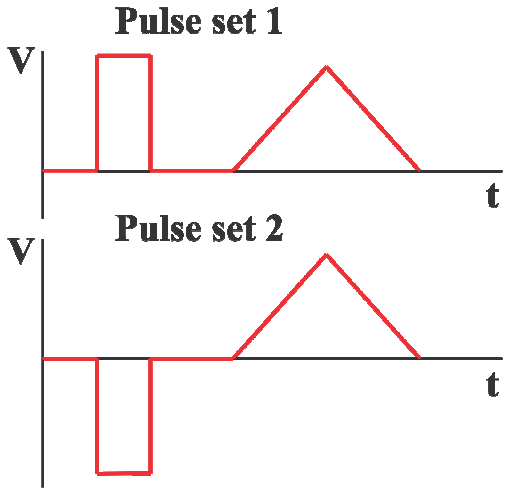

Figure S3. Pulse trains for measurements of the remanent polarization loops.